Water Cycle Intensification: A Complementary Approach

Mijael Rodrigo Vargas Godoy[a, 1] **and Yannis Markonis**[a]

[a]Faculty of Environmental Sciences, Czech University of Life Sciences Prague, Kamýcká 129, Praha – Suchdol, 165 00, Czech Republic

The difference between precipitation and evaporation has been extensively used to characterize the water cycle's response to global warming. However, when it comes to the global scale, the information provided by this metric is inconclusive. Herein, we discuss how the sum of precipitation and evaporation could complement the assessment of global water cycle intensification. To support our argument, we present a brief yet robust correlation analysis of both metrics in four reanalysis data sets (20CR v3, ERA-20C, ERA5, and NCEP/NCAR R1). Additionally, by combining the two metrics, we investigate how well the global water cycle fluxes are represented in the four reanalyses. Among them, we observe four different responses to the temperature increase between 1950-2010, with ERA5 showing the best agreement with the intensification hypothesis. We argue that these discrepancies would remain elusive with the traditional approach, which makes the utilization of the sum of precipitation and evaporation a valuable addition to our methodological toolbox for the assessment of the global water cycle intensification.

Global Water Cycle | Water Cycle Intensification | Hydrological Cycle Acceleration | Climate Reanalysis | ERA5

U nderstanding the global water cycle and its balance is crucial for Earth system science and climate change studies. To assess the water cycle at multiple spatiotemporal scales, we observe and measure the fluxes and storage that comprise its budget. Over land, the net water flux into the surface, a vital aspect of the water cycle for human society, is described by the difference between precipitation and evaporation ($P - E$). Thus, $P - E$ characterizes atmosphere-land surface interactions and represents the maximum available renewable freshwater (1). Therefore, it is not uncommon to study the behavior of this compound variable rather than solely precipitation or evaporation. Analogously, evaporation minus precipitation ($E - P$) determines the surface salinity of the ocean, which helps determine the stability of the water column (2). These two formulations, i.e., $P - E$ and $E - P$, are the most used metrics to assess the current state and future changes of the water cycle (3).

Consequently, it is no surprise that there have been numerous efforts to accurately describe the spatiotemporal patterns of $P - E$. There is a consensus that as precipitation increases over land, so does the evaporation over the oceans to balance the global water cycle (4). As a result, standardized $P - E$ over land and the oceans should mirror each other, suggesting that the precipitation and evapotranspiration offset over land is balanced by the evaporation and precipitation offset over the oceans. Notwithstanding, it has become increasingly evident that there are contrasting responses between the terrestrial and oceanic water cycles (5). Furthermore, upscaling into the global scale and regarding the interannual and longer temporal scales, mean precipitation and evaporation are roughly on par (6), making $P - E$ close to or equal to zero, which unavoidably

adds little to no value when evaluating long-term changes in the global water cycle. Hence, the insight gained from $P - E$ on water cycle research appears to be limited by the scale at which it is assessed.

A plausible alternative worth exploring is to use $P + E$ as a complementary metric to assess water cycle variations. At the regional scale, for example, moisture convergence can increase precipitation (7). Assuming radiation is not limiting, evapotranspiration will be equally enhanced. On the one hand, $P - E$ would suggest no change in the hydrological cycle, while, on the other hand, the increase in $P + E$ would correctly indicate that the water cycle is indeed changing, with more water being circulated in total through the surface-atmosphere continuum. Huntington et al. (8) have already shown that the sum of precipitation and evapotranspiration can be adequately applied to quantify the changes in the terrestrial portion of the water cycle. We argue that this approach can be extended to the description of the whole water cycle because $P + E$ has a robust physical meaning; it describes the total flux of water exchanged between the atmosphere and the surface. Furthermore, like the human heart, the Earth cycles far more water through the atmosphere than its holding capacity. In this manner, it would make sense to also look into the addition of fluxes rather than only their difference when assessing global water cycle intensification.

In this study, we physically define precipitation plus evaporation as a metric to explore its potential to complement research on water cycle changes at the global scale. The data

---

Significance Statement

Estimating precipitation minus evaporation has helped evaluate different aspects of the water cycle, such as the changes in response to global warming at multiple scales. However, the information we gain from this metric becomes limited on a global scale. This work proposes implementing the sum of precipitation and evaporation in a complementary approach. Our assessment revealed that precipitation plus evaporation comprehensively describes the relationship between the water cycle and temperature. By combining this complementary metric to precipitation minus evaporation, we can better assess how the global water cycle is presented in reanalyses and earth system models. As a result, we can improve the evaluation of their performance and enhance our understanding of the water cycle changes on a global scale.

www.pnas.org/cgi/doi/10.1073/pnas.XXXXXXXXXX

PNAS | July 11, 2022 | vol. XXX | no. XX | 1–6

sources we rely on for such research have continuously evolved, but even the most extensive ground observational networks cover only about 1% of Earth's surface (9). In pursuit of a more exhaustive assessment at the global scale, we relied on reanalysis data to evaluate both $P + E$ and $P - E$. First, we compare both metrics' aptness to comprehensively capture the global water cycle's response to global warming, and we evaluate the $P + E$ behavior in terms of hydrological sensitivity. Then, we present the application of $P + E$ in a framework that describes the changes in the water cycle. We achieve this by exploring the changes in atmospheric water fluxes and storage redistribution between land-ocean and the atmosphere, as well as the mean temperature conditions. Finally, we discuss the possible connotations of the findings regarding $P + E$ and its application as a performance metric for reanalysis data.

The Physical Basis

The proposed framework is based on quantifying precipitation, evaporation, their difference, and their sum. The latter, precipitation plus evaporation, is mathematically complementary to the widely used $P - E$ metric. Nonetheless, math alone does not suffice to improve our understanding of the global water cycle. Thus, we will define $P + E$ from a mass balance and a kinematic perspective.

Water Cycle Budget. The global water cycle's mass balance is expressed with the water budget equation:

$$P + Q_{\text{in}} = E + Q_{\text{out}} + \Delta S \tag{1}$$

where P is precipitation, Q_{in} is water flow into the Earth, E is evaporation (since we are at the global scale we will refer to it simply as evaporation for brevity, but we acknowledge it encompasses evaporation from soils, surface-water bodies, and plants), ΔS is water storage change in the land-ocean continuum (biological water, fresh lakes, ice, nonrenewable groundwater, oceans, permafrost, reservoirs, renewable groundwater, rivers, saline lakes, seasonal snow, soil moisture, and wetlands), and Q_{out} is water flow out of the Earth. All terms are averaged globally over a fixed time period (e.g., $[mm/yr]$). At the global scale, due to Earth's gravity and temperature, water inflow or outflow leaking between the atmosphere and outer space is negligible compared with precipitation and evaporation and water storage change (10). Consequently, $Q_{in} \to 0$ and $Q_{out} \to 0$ leaving us with:

$$\Delta S = P - E \tag{2}$$

where ΔS represents a storage redistribution from the atmosphere towards the land-ocean continuum (positive), from the land-ocean continuum towards the atmosphere (negative), or steady state equilibrium (zero). Now, we define global water cycle intensity as:

$$\text{GWCI} = P + E \tag{3}$$

In this manner, intensity is defined as the total total flux of water exchanged between the atmosphere and the land-ocean continuum. This definition is in line with previous formulations in the literature (8, 11). Furthermore, different ways to integrate precipitation and evaporation to describe the hydroclimatic regime have been in use since for over half a century now (e.g., Budyko curve (12)).

Water Cycle Kinematics. As established above, precipitation plus evaporation describes the water cycle intensity from a mass balance perspective by quantifying the total flux of water exchanged between the atmosphere and the land-ocean continuum. If we describe these atmospheric water fluxes from a kinematic perspective, we have two velocity vectors:

$$\vec{P} = \mathbf{P}(x, y, \hat{z})$$
$$\vec{E} = \mathbf{E}(x, y, -\hat{z}) \tag{4}$$

where $\mathbf{P}$ is precipitation rate and $\mathbf{E}$ is evaporation rate at any location on Earth's surface. These velocities are parallel to each other but are oriented in opposite directions. Precipitation and evaporation are heavily intertwined through moisture recycling. Therefore, we could characterize their interdependence relationship by defining the velocity of the global water cycle as the Newtonian relative velocity of precipitation with respect to evaporation:

$$\begin{aligned} \overrightarrow{GWC} &= \vec{P} - \vec{E} \\ &= \mathbf{P}(x, y, \hat{z}) - \mathbf{E}(x, y, -\hat{z}) \\ &= (\mathbf{P} + \mathbf{E})(x, y, \hat{z}) \end{aligned} \tag{5}$$

where $(\mathbf{P} + \mathbf{E})$ is the magnitude of global water cycle velocity. Hence, we can safely ascertain that assessing changes in $P + E$ refers to acceleration or deceleration of the global water cycle.

Results

Our analyses, taken together, show the untapped research potential of precipitation plus evaporation to complement water cycle intensification research. We start by revealing the standing of $P + E$ with $P - E$ as the existing reference. The added value of the $P + E$ metric becomes readily visible by the superimposition of the annual mean global temperature and the annual total global $P + E$ of the four reanalysis data sets (Figure 1). Their coupling is statistically supported by quantifying the linear relationship between these variables (Table 1). The dominant behavior in the long-term relationships reports three common markers: a strong $P + E$ correlation (R-squared ≈ 0.8; Figures 1B, 1D, and 1F), a very weak $P - E$ correlation (R-squared < 0.2; Figures 1A, 1C, and 1G), and an apparent decoupling between $P + E$ and temperature around the 1960s. We observe particular traits for ERA5 and NCEP/NCAR R1. ERA5 shows a moderate yet inverse $P - E$ correlation (R $= -0.63$; Figure 1E). NCEP/NCAR R1, not resembling the other three data sets, has a higher correlation for the difference than the sum of precipitation and evaporation(0.18 vs 0.12 R-squared). Moreover, the coupling between $P + E$ and temperature occurs only after the mid-1970s (Figure 1H). The robust performance of $P + E$ over $P - E$ as a metric to substantiate the relationship between atmospheric water fluxes and temperature carries from the long-term onto the year-to-year variability (Table 1). Estimating the annual differences, we now observe a homogeneous behavior in all the reanalyses data sets with moderate $\delta(P + E)$ correlation (R-squared between $0.19 - 0.37$) and no $\delta(P - E)$ correlation (R-squared ≤ 0.02). This independence in $\delta(P - E)$ imply that the correlation observed between $P - E$ and temperature was due to the long-term trends, while $P + E$ correlates both to short-term and long-term temperature variability.

Thermodynamics, Clausius–Clapeyron scaling in particular, determine the relationship between atmospheric water vapor
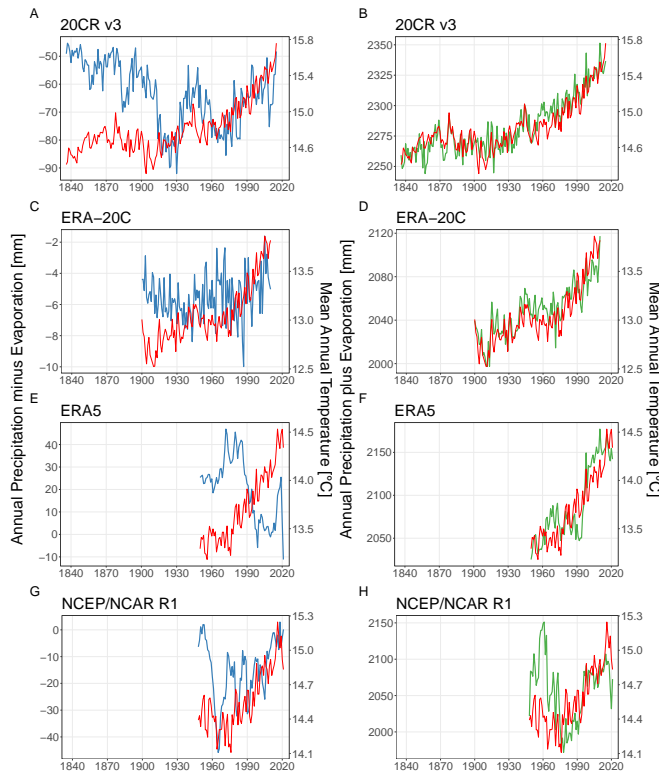
Fig. 1. Average global atmospheric water fluxes in $[mm/year]$ and temperature in $[^\circ C]$, where P is precipitation, E is evaporation, and T is temperature. $P + E$ in green, $P - E$ in blue, and temperature in red.

and temperature. However, it is the Earth's energy balance that governs global precipitation and evaporation, and constraining the hydrological sensitivity (3). Consequently, $P + E$ should also increase at approximately 2-3 $[\%/^\circ C]$. To validate our hypothesis, we looked into the slopes of linear regression fits between $P + E$, P, and temperature (Table 2). We validated the anticipated increases for $P + E$ except for ERA5, which had a rate of 4.9 ± 0.3 $[\%/^\circ C]$, but also a rather high precipitation increase of 3.8 ± 0.3 $[\%/^\circ C]$. R-squared offers some insight about the proportion of variance in $P + E$ and P that can be explained by temperature. In general the differences were quite low. 20CR v3 and ERA5 have higher R-squared values for $P + E$ than for P, with differences of 0.12 and 0.09, respectively. In contrast, ERA-20C and NCEP/NCAR R1 have higher R-squared values for precipitation (0.01 and 0.05). Note that while precipitation has a higher R-squared for ERA-20C and NCEP/NCAR R1, the difference is one order of magnitude smaller than those whose $P + E$ has a higher

R-squared (20CR v3 and ERA5). These results demonstrate a good coupling between $P + E$ and hydrological sensitivity.

The above analysis highlights the differences between $P - E$ and $P + E$. We will now show their complementary value through a graphical framework that integrates precipitation, evaporation, their difference, and their sum. By transforming the changes in the relationship of P and E to changes in $P - E$ and $P + E$, we can describe the water cycle dynamics in terms of atmospheric water storage and fluxes correspondingly. We apply this procedure to the four reanalyses to explore their representation of water cycle between two 30-year periods (1951-1980 and 1981-2010; Figure 2). It is easy to pinpoint some distinguishable features for each data set. The 20CR v3 appears to have substantially higher atmospheric water flux estimates than any other reanalysis. However, if we decompose it in $P - E$ and $P + E$ terms, we can see that in the two periods examined, the difference between precipitation and evaporation increased (blue vector), implying atmospheric water loss (Figure 2B). In ERA5, the exact opposite behavior emerges. The atmospheric water content has been increasing, but overall the average conditions suggest that the atmosphere has been getting drier since 1950 (Figure 2D). The remaining two reanalyses manifest a stationary relationship in the water storage with no changes in the $P - E$ component (Figures 2C and 2E). Surprisingly, the flux of atmospheric water is decreasing in NCEP/NCAR R1, suggesting a weakening of the water cycle (green arrow; Figure 2C).

It is evident that no two reanalyses are alike when it comes to the exchange of water between the land-ocean continuum and the atmosphere at the global scale. In terms of magnitude, ERA5 reports changes in $P + E$ accelerating almost twice as fast as in the 20CR v3 and ERA-20C (41.5 $[mm/yr]$ versus 23.69 $[mm/yr]$ and 25.3 $[mm/yr]$, respectively). The $P + E$ change in NCEP/NCAR R1 is similar to that observed in the 20CR v3 and ERA-20C. Although as already mentioned, in the opposite direction. Looking beyond 1950, in the reanalyses with longer records (20CR v3 and ERA-20C), we can see an agreement in the direction of change since 1921. Additionally, both reanalyses show a higher increase in $P + E$ between 1951-1980 and 1981-2010 than between 1921-1950 and 1951-1980. What is different, though, is the behavior of $P - E$, especially if analyzed over their 30-year average trajectory (Figures 2B and 2C; light grey points). In ERA-20C, $P - E$ changes remain consistently stationary and very close to zero (0.15 $[mm/yr]$), while in the 20CR v3 oscillates substantially following both acceleration and deceleration patterns over the last 120 years. The trajectories of the other two reanalyses show behaviors somewhere in between, with more flexibility in $P - E$ compared to ERA-20C but not as much freedom

Table 1. Atmospheric water fluxes vs. temperature long-term and year-to-year linear relationships, where P is precipitation, and E is evaporation.

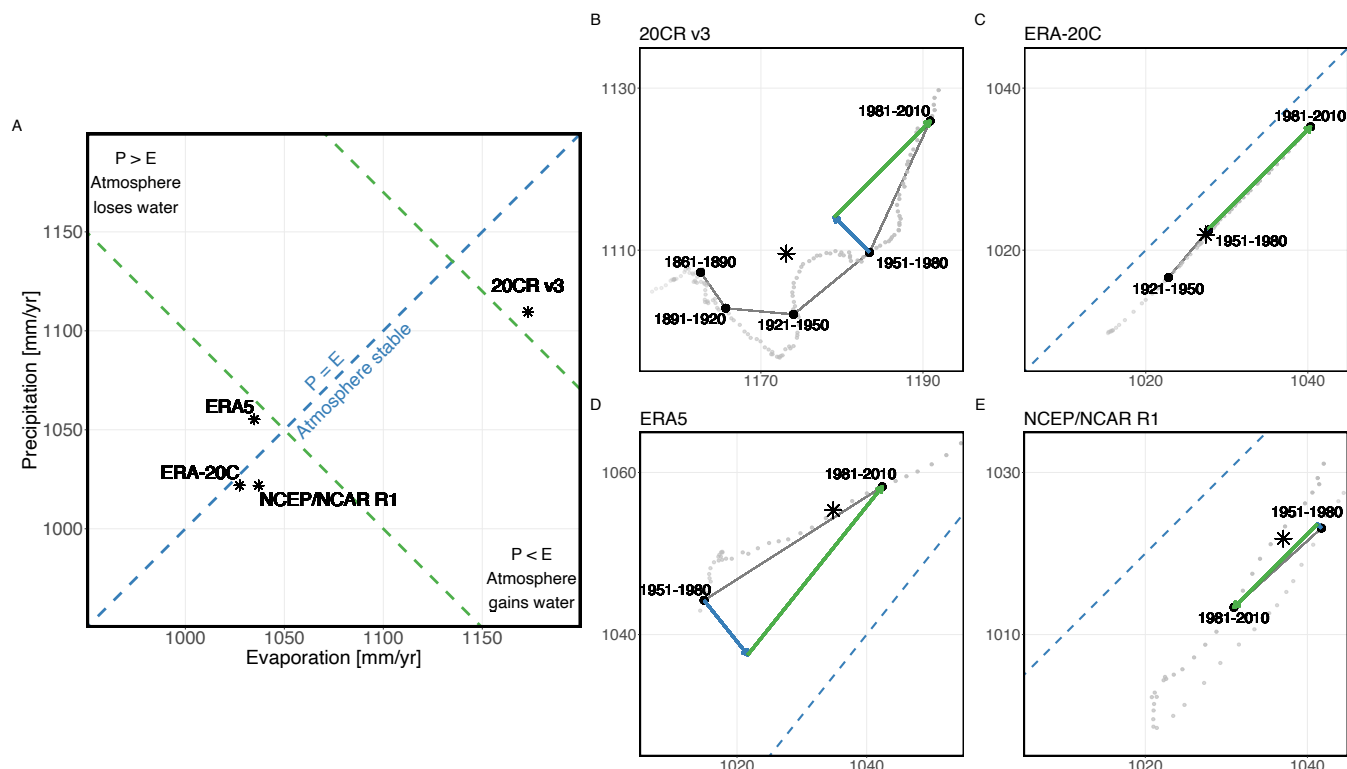| | Long-term | | | | Year-to-year | | | |
| | $P + E$ | | $P - E$ | | $\delta(P + E)$ | | $\delta(P - E)$ | |
Reanalysis	R-squared	p-value	R-squared	p-value	R-squared	p-value	R-squared	p-value
20CR v3	0.82	$< 2 \times 10^{-16}$	0.01	0.14	0.19	1×10^{-9}	2×10^{-4}	0.87
ERA-20C	0.80	$< 2 \times 10^{-16}$	0.06	1×10^{-2}	0.37	2×10^{-12}	0.02	0.15
ERA5	0.75	$< 2 \times 10^{-16}$	0.39	3×10^{-9}	0.35	3×10^{-8}	0.02	0.20
NCEP/NCAR R1	0.12	2×10^{-3}	0.18	2×10^{-4}	0.22	2×10^{-5}	4×10^{-3}	0.58

Fig. 2. Graphical framework for the assessment of global water cycle intensification. P and E are global precipitation and evaporation in $[mm/year]$. Contour of $P = E$ is shown as a blue dashed line. Contours of equal $P + E$ are shown as green dashed lines. Changes in $P - E$ and $P + E$ are shown as blue and green vectors correspondingly. (A) Relationship between average P and E for the full record of reanalyses. (B) Zoomed in panel on the 20CR v3. (C) Zoomed in panel on ERA-20C. (D) Zoomed in panel on ERA5. (E) Zoomed in panel on NCEP/NCAR R1.

as in the 20CR v3. Overall, the combination of $P - E$ and $P + E$ revealed a wealth of additional information about the reanalyses performance that is easily communicable and reproducible, shaping the path for further investigations into the reasons behind these differences.

Discussion

The overall results suggest that $P + E$ holds promise to overcome the scale limitations of $P - E$ and complement global water cycle research within the framework proposed. Most significantly, including $P + E$ revealed additional information about the intensification characteristics in four reanalyses (Figure 2). Whilst some features were common for all or most reanalyses, like changes in $P - E$ being much smaller than in $P + E$, we observed various individual distinctions. Although it is not the scope of this study to investigate the reasons behind the discrepancies among reanalyses, looking into them offers a handy demonstration of what can be learned by utilizing this

metric to assess water cycle intensification.

Out of the four reanalyses, ERA5 was found to represent better the intensification dynamics between 1951-1980 and 1981-2010. At the same time, ERA5 has the most pronounced changes for $P - E$, showcasing improvements in its terrestrial water storage computations (13). However, ERA5 has has the steepest acceleration of $P + E$ and is the only reanalysis above the $P = E$ isoline for the entirety of its record, which could be an artifact attributed to precipitation overestimations identified across different regions (14). To the opposite end, NCEP/NCAR R1 shows a decline in atmospheric water fluxes over time with a slight decrease in atmospheric water storage. Forbye, the 30-year average trajectory exhibits an acute u-turn between the mid-1960s and the late 1970s. Before and after this trajectory inversion, the behavior is similar to ERA-20C with little to no variability along a $P - E$ isoline.

In addition, the simple superimposition of annual mean global temperature and annual total global $P + E$ indicated

Table 2. Comparison of $P + E$ vs. T and P vs. T linear relationships, where P is precipitation, E is evaporation, T is temperature, and RSE is Residual Standard Error.

Reanalysis	Record	$P + E$		P	
		slope [%/°C]	RSE	slope [%/°C]	RSE
20CR v3	1836 - 2015	3.2 ± 0.1	0.43	3.1 ± 0.2	0.59
ERA-20C	1900 - 2010	3.3 ± 0.2	0.51	3.3 ± 0.2	0.50
ERA5	1950 - now	4.9 ± 0.3	1.04	3.8 ± 0.3	0.99
NCEP/NCAR R1	1948 - now	2.8 ± 0.9	2.0	4 ± 1	2.2

an apparent decoupling of $P + E$ and temperature before the late 1970s for the NCEP/NCAR R1 reanalysis (Figure 1H). A possible explanation for this abnormal behavior could be traced back to remote sensing data assimilation. Inconsistencies in its atmospheric data pre-1979 have previously been reported and associated with the lack of satellite observations before 1979, e.g., in the Southern Hemisphere (15). Further evidence of early record inconsistencies on NCEP/NCAR R1 arises when reckoning the year-to-year correlation, removing long-term trend biases, as its R-squared value doubled for $P + E$ (Table 2). Another point of interest from Figure 1 is the pinpointed decoupling of $P + E$ and temperature visible around the 1960s, which coincides with a shift in the direction of global terrestrial near-surface wind speed changes (increasing trend before 1967 and decreasing after that (16)).

Using solely $P + E$ comes with its own limitations and could mask the true dynamics of global water cycle change. The reciprocal complementarity of $P + E$ and $P - E$ is better perceived on the long-record reanalyses. The overview clearly shows that the 20CR v3 portrays a warmer and wetter Earth relative to the rest of the reanalyses. This is consistent with biases in the vertical structure of mass and circulation determined throughout the atmosphere (17). Having said that, the magnitude of changes in $P + E$ are consistent with those of ERA-20C. The most recent increase is higher than the preceding ones and suggests that the global water cycle intensification signal has further strengthened in the last three decades (18). The above would suggest that changes in the global water cycle are similarly represented on both data sets. In sooth, $P - E$ changes in the 20CR v3 oscillate substantially following both acceleration and deceleration patterns, whereas ERA-20C shows little to no variability and steadily moves along a $P - E$ isoline. Reportedly, there are only subtle differences in the data assimilated and the data assimilation schemes between these two reanalyses (19), yet we can see contrasting behaviors exposed within the framework proposed herein.

Our findings, including the good agreement with the range of hydrological sensitivity, advocate for the definitions of $P + E$ to be physically sound. It is important, nonetheless, to note that such an agreement is not a two-way relationship. As seen in our examination, the fact that all the reanalyses have similar hydrological sensitivities does not necessarily mean that they express a similar rate of water cycle intensification. Assuming so could be misleading, whereas we can get more insight and avoid these pitfalls by decomposing the change into $P - E$ and $P + E$ (i.e., into water storage and fluxes). It could be argued that introducing a new metric for intensification into the current broad spectrum of metrics may lead to inconsistent hydroclimatology studies terminology, such as that recently reported for wetter and drier (20). Nevertheless, $P + E$ is not just an index because it is physically grounded and, as such, is better suited to describe climate models and reanalyses (21). Furthermore, by physically defining $P + E$ from a water cycle mass balance and kinematics outlook, we bridge the gap between the terms of global water cycle "intensification" and "acceleration".

The above applications highlight the potential of $P + E$ to complement water cycle research at the global scale. The proposed framework could advance our understanding of water cycle intensification and improve climate modeling. We have already revealed some discrepancies between the reanalysis data sets. Further analyses using observational data sets could determine if the strong coupling between $P + E$ and temperature is not an artifact of the reanalysis process. Still to achieve this, the observational limitations at global scale, especially in evaporation, need to be overcome (22). Additionally, it is intriguing to see how the total water transfer between the land-ocean continuum and atmosphere appears in Earth System Models and whether it can be also applied as a metric for the model performance. Future research into global spatial patterns of $P + E$ could also shed more light on how they relate to regional changes and hydroclimatic extremes such as droughts. To this extent, quantifying the surface-atmosphere water exchange in the form of $P + E$ can enhance our insight into past, present, and future hydroclimatic variability.

Materials and Methods

We examined different statistical metrics commonly used in time-series analyses to benchmark the complementary metric $P + E$ against the traditional $P - E$. For superimposing the temperature to $P + E$ and $P - E$ time series (Figure 1) we matched the maximum and minimum values and then multiplied it by the ratio of their differences. I.e.,

$$y' = \left((T - min(T)) * \frac{max(P \pm E) - min(P \pm E)}{max(T) - min(T)} \right) + min(P \pm E)$$

As thermodynamics dictates, we expect a linear relationship between atmospheric water fluxes and temperature. This correspondence was quantified via the square of the Pearson correlation coefficient and its statistical significance via the p-value. The same metrics were computed again for the annual differences of each time series. To this extent, we can characterize the long-term and the year-to-year association between atmospheric water fluxes and temperature. While the correlation coefficient describes the presence or absence of a linear relationship, it does not quantify the rate of change of one variable relative to the other. Henceforth, we used linear regression to estimate the corresponding slopes and describe the rate of change at which atmospheric water fluxes respond to changes in temperature. To compare the slopes between data sets on a one-to-one basis, we estimated atmospheric water fluxes and temperature in terms of global anomalies with respect to the 1981-2010 period. We relied on the residual standard error to assess the goodness-of-fit of the slopes, i.e., how well these slopes represent the linear relationship between our variables.

The above examination highlighted the differences between the metric proposed herein $P + E$ and the widely used $P - E$. However, this comparison was not in pursuit of presenting $P + E$ as a replacement but as a complement to achieve a more comprehensive framework. Including precipitation, evaporation, their difference, and their sum provides a synthesized visual of the overall response of the water cycle to global warming similar to that described by Huntington et al. (8). The global water cycle regimes in this framework would be described by their precipitation and evaporation coordinates, and vectors represent changes between two periods (Figure 3). Precipitation and evaporation may increase, decrease, or remain constant. From equation [2], changes in atmospheric water storage ($P - E$) shown as blue contours are planes that increase from the bottom right (wetter) to the top left corner (drier). It is important to note that Huntington et al. (8) focused on soil water storage, as such the directions for drier and wetter are reversed therein. From equation [3], water cycle intensity ($P + E$) is a plane shown as green contours that increases from the bottom left (cooler) to the top right (warmer). $P - E$ is negative to the right of the identity diagonal, zero along this line, and positive to the left of the line. At the global scale, negative values describe an increase in atmospheric water storage (wetter), positive values describe an increase in land-ocean water storage (drier), and zero describes steady-state equilibrium. $P + E$ increases describe shifts from cooler regimes into warmer ones.
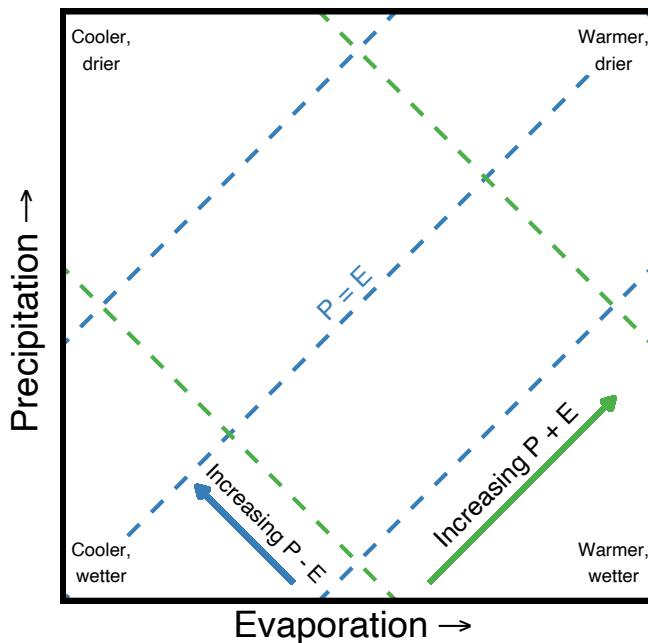
Vargas Godoy *et al.*

PNAS | **July 11, 2022** | vol. XXX | no. XX | **5**

Fig. 3. Vector representation of global water cycle response to global warming, where P is precipitation, and E is evaporation. Contours of equal $P - E$ are shown as blue dashed lines. Contours of equal $P + E$ are shown as green dashed lines.

Data. We selected four reanalysis data products based on the availability of precipitation, evaporation, and temperature for a given data set (Table 3). These are the Twentieth Century Reanalysis (20CR) v3 (23), European Centre for Medium-Range Weather Forecasts (ECMWF) Reanalyses ERA-20C (19) and ERA5 (24), and the National Centers for Environmental Prediction & the National Center for Atmospheric Research NCEP/NCAR Reanalysis 1 (25). The 20CR v3 estimates assimilate only surface observations of synoptic pressure into NOAA's Global Forecast System throughout the 19th and 20th centuries. ERA-20C is ECMWF's first atmospheric reanalysis of the 20th century, reaching 2010. It assimilates observations of surface pressure and surface marine winds only. ERA5 has replaced the ERA-Interim reanalysis, which stopped on 31 August 2019, and covers 1950-present. It combines vast amounts of historical observations into global estimates using advanced modeling and data assimilation systems. The NCEP/NCAR R1 project uses a state-of-the-art analysis/forecast system to perform data assimilation using past data from 1948 to the present. All of the above data sets are available for download at KNMI Climate Explorer (climexp.knmi.nl), as well as on the dedicated websites of their providers. Through the KNMI Climate Explorer we generated annual values for total atmospheric water fluxes and global mean temperature.

Data Availability. The data generated herein and the R scripts for the figures presented in the study are publicly available at github.com/MiRoVaGo/P_plus_E

1. T Oki, S Kanae, Global hydrological cycles and world water resources. *science* **313**, 1068–1072 (2006).
2. L Yu, SA Josey, FM Bingham, T Lee, Intensification of the global water cycle and evidence from ocean salinity: a synthesis review. *Annals New York Acad. Sci.* **1472**, 76–94 (2020).
3. RP Allan, et al., Advances in understanding large-scale responses of the water cycle to climate change. *Annals New York Acad. Sci.* **1472**, 49–75 (2020).
4. IM Held, BJ Soden, Robust responses of the hydrological cycle to global warming. *J. climate* **19**, 5686–5699 (2006).
5. MP Byrne, PA O'Gorman, The response of precipitation minus evapotranspiration to climate warming: Why the "wet-get-wetter, dry-get-drier" scaling does not hold over land. *J. Clim.* **28**, 8078–8092 (2015).
6. AG Pendergrass, DL Hartmann, The atmospheric energy constraint on global-mean precipitation change. *J. climate* **27**, 757–768 (2014).
7. V Espinoza, DE Waliser, B Guan, DA Lavers, FM Ralph, Global analysis of climate change projection effects on atmospheric rivers. *Geophys. Res. Lett.* **45**, 4299–4308 (2018).
8. TG Huntington, PK Weiskel, DM Wolock, GJ McCabe, A new indicator framework for quantifying the intensity of the terrestrial water cycle. *J. Hydrol.* **559**, 361–372 (2018).
9. MR Vargas Godoy, Y Markonis, M Hanel, J Kyselý, SM Papalexiou, The global water cycle budget: A chronological review. *Surv. Geophys.* **42**, 1075–1107 (2021).
10. DC Catling, KJ Zahnle, The planetary air leak. *Sci. Am.* **300**, 36–43 (2009).
11. PK Weiskel, et al., Water use regimes: Characterizing direct human interaction with hydrologic systems. *Water Resour. Res.* **43** (2007).
12. MI Budyko, *Climate and life.* (Academic Press, Inc.), (1974).
13. A Eicker, et al., Daily grace satellite data evaluate short-term hydro-meteorological fluxes from global atmospheric reanalyses. *Sci. reports* **10**, 1–10 (2020).
14. B Hassler, A Lauer, Comparison of reanalysis and observational precipitation datasets including era5 and wfde5. *Atmosphere* **12**, 1462 (2021).
15. W Tennant, Considerations when using pre-1979 ncep/ncar reanalyses in the southern hemisphere. *Geophys. Res. Lett.* **31** (2004).
16. C Shen, et al., Estimating centennial-scale changes in global terrestrial near-surface wind speed based on cmip6 gcms. *Environ. Res. Lett.* **16**, 084039 (2021).
17. L Slivinski, et al., An evaluation of the performance of the twentieth century reanalysis version 3. *J. Clim.* **34**, 1417–1438 (2021).
18. P Greve, et al., Global assessment of trends in wetting and drying over land. *Nat. geoscience* **7**, 716–721 (2014).
19. P Poli, et al., Era-20c: An atmospheric reanalysis of the twentieth century. *J. Clim.* **29**, 4083–4097 (2016).
20. N Roth, et al., A call for consistency with the terms 'wetter'and 'drier'in climate change studies. *Environ. Evid.* **10**, 1–7 (2021).
21. KA McColl, ML Roderick, A Berg, J Scheff, The terrestrial water cycle in a warming world. *Nat. Clim. Chang.* (2022).
22. MF McCabe, et al., The gewex landflux project: Evaluation of model evaporation using tower-based and globally gridded forcing data. *Geosci. Model. Dev.* **9**, 283–305 (2016).
23. LC Slivinski, et al., Towards a more reliable historical reanalysis: Improvements for version 3 of the twentieth century reanalysis system. *Q. J. Royal Meteorol. Soc.* **145**, 2876–2908 (2019).
24. H Hersbach, et al., The era5 global reanalysis. *Q. J. Royal Meteorol. Soc.* **146**, 1999–2049 (2020).
25. E Kalnay, et al., The ncep/ncar 40-year reanalysis project. *Bull. Am. meteorological Soc.* **77**, 437–472 (1996).

Table 3. Data Set Overview as Available at KNMI Climate Explorer

Data Set	Spatial Resolution	Record Length	Reference
20CR v3	1°	1836 - 2015	(23)
ERA-20C	1.125°	1900 - 2010	(19)
ERA5	0.25°	1950 - now	(24)
NCEP/NCAR R1	1.875°	1948 - now	(25)